

**Proceedings of the 16th International Conference on Nuclear Engineering
ICONE16
May 11-15, 2008, Orlando, Florida, USA
ICONE16-48438**

**VALIDATION OF CFD METHODS USING DATA FOR A VENTILATED DRY STORAGE
CASK**

Abdelghani Zigh

US Nuclear Regulatory Commission
11545 Rockville Pike, Rockville, MD 20852

Jorge Solis

US Nuclear Regulatory Commission
11545 Rockville Pike, Rockville, MD 20852

ABSTRACT

Measured temperature data obtained from a spent fuel dry cask under long term storage conditions are used to validate computational fluid dynamics (CFD) methods. CFD methods are currently being used by dry cask vendors to design and analyze spent fuel storage and transportation casks. To gain a better understanding of CFD's capabilities to analyze the complex heat transfer and flow phenomena occurring in a passive dry cask system, a three-dimensional CFD model was developed and validated using data for a ventilated storage cask (VSC-17) collected by Idaho National Laboratory (INL). The developed Fluent CFD model was validated to minimize modeling and application uncertainties. To address modeling uncertainties, the report focused on turbulence modeling of buoyancy driven air flow. Similarly, in the application uncertainties, the pressure boundary conditions used to model the air inlet and outlet vents were investigated and validated. The VSC-17 consisted of 17 consolidated cells loaded with consolidated PWR spent fuel. At the time of the tests, the fuel was generating about 15 kW of decay heat. The experimental tests were performed with vacuum, nitrogen and helium backfill environments in a vertical orientation. Measured cask surface, concrete, air channel surfaces, and fuel canister guide tube temperature data were compared to Fluent CFD predictions.

Different turbulence models were used to reduce the modeling uncertainty in the CFD simulation of the air flow through the annular gap between the overpack and the multi-assembly sealed basket (MSB). Among the chosen turbulence models, the validation

showed that the low Reynolds $k-\epsilon$ and the transitional $k-\omega$ turbulence models predicted the measured temperatures closely and compared well. To assess the impact of pressure boundary conditions used at the air inlet and outlet channels on the application uncertainties, a sensitivity analysis of operating density values was undertaken. The validation showed that the correct operating density corresponds to the density evaluated at the air inlet condition of pressure and temperature.

INTRODUCTION

This paper addresses two categories of uncertainties, with specific guidelines to minimize them. The first category is modeling uncertainties. These uncertainties are due to the difference between the real flow and the approximate solution of the model equations. This paper provides an independent verification and validation of the modeling approach used to model the heat transfer and fluid flow in a dry cask to reduce modeling uncertainties. In particular, the discussion of modeling uncertainties focused on the turbulence modeling which can greatly influence the final results if not applied correctly. Fluent has many turbulence models that are not generalized and, therefore, can not be applied to all types of flows. Depending on the complexity of the flow, some models are more suited than others. In this paper, several approaches to model air flow turbulence have been investigated and compared to experimental data. The paper suggests CFD best practice guidelines to minimize turbulence modeling uncertainties in the dry cask analysis.

*** The opinions expressed in this paper are strictly those of the authors and do not constitute official U.S Nuclear Regulatory Commission opinion.

The second category of uncertainty is the application uncertainties. These uncertainties are introduced because the application is complex and precise data needed for the simulation is not always available. In this paper, the discussion of application uncertainties focused on the inlet and outlet boundary conditions of cooling air. In a ventilated dry cask, as cooling air is naturally induced, pressure boundaries were the preferred choice at the air inlet and outlet ducts. The pressure gradient in the air flow channel affects the magnitude of the potential buoyancy forces due to the heat source (i.e. decay heat) and as such, these pressure boundary conditions are very crucial to the uncertainties that can be introduced in the simulation. In this paper, the effect of the pressure boundary conditions was investigated and compared to the experimental data to minimize the application uncertainties. This paper gives specific guidelines to avoid application uncertainties that could arise in the specification of the pressure boundary conditions at the air inlet and outlet ducts of the dry cask.

Experimental data previously obtained for a ventilated storage cask were used for the validation. To reduce modeling uncertainties, different turbulence models were used and compared to the experimental data. The low Reynolds $k-\epsilon$ turbulence model was found to give very satisfactory results. To reduce the application uncertainties, sensitivity analyses using different pressure gradients by varying the operating density were performed. Comparison to the experimental data showed that the correct operating density corresponded to the density evaluated at the air inlet conditions of pressures and temperatures.

The flow regime for air flow and helium flow is an important parameter that can affect the analysis. The assumption of fully turbulent flow inside and outside the canister, will lead to a lower Peak Cladding Temperature (PCT). On the other hand, assuming laminar flow inside and outside the canister would lead to a higher PCT. As such, careful and correct characterization of the flow regime is required to avoid mis-prediction of the flow variables. In the present analysis, different turbulence models were used to model the air flow in the dry cask cooling channel. Four models were used covering the low and high range of Reynolds number as well as the transitional range. In addition to standard $k-\epsilon$ model and laminar flow models, low Reynolds $k-\epsilon$, and transitional $k-\omega$ Shear Stress Transport (SST) models were used. The standard $k-\epsilon$ model is suited to model

high Reynolds fully-developed turbulent flows, while low Reynolds $k-\epsilon$ and transitional $k-\omega$ SST models are adequate to model flows in low, transitional, and high Reynolds range.

Pressure boundaries are used to model heat and flow in the dry cask. One issue that arose while using pressure boundary conditions at the inlet and exit of the dry cask is the operating density. This parameter has major effect on the results, and should be used properly. To assess the use of the pressure boundary conditions, two types of control volumes were used to perform the analysis. One choice was to include part of the outside ambient to the dry cask. Hence, the inlet and outlet vents will not be part of the specified boundary. Instead, the inlet and outlet channels will be part of the computational domain. In the second choice, the boundaries of the cask were used as a boundary of the modeled control volume. At the start, the first control volume results were used to validate the inlet boundary conditions (i.e. inlet temperature) to the second control volume. Operating density is an input parameter to Fluent and will be of great importance to the final results when pressure boundaries are used as shown in [Fluent, 2006]. According to the Fluent user manual, the operating density should be representative of the volumetric average density of the fluid. In the extended control volume, the air volume consists, in big part, of the chosen isothermal ambient volume and the negligible volume of air cooling the canister in the air gap between the canister and liner walls. Therefore, for the extended control volume case, the operating density will be equal to that of the ambient. When the second control volume is chosen, the fluid volume consists of only the air flowing in the air gap which is getting warmed as it goes up. According to [Fluent, 2006], the operating density in this case is equal to the volumetric average density of the column of air between the inlet and the outlet ducts.

Description of the VSC-17 Experiments

The VSC-17 spent fuel storage system is a passive heat dissipation system for storing 17 assemblies of consolidated spent nuclear fuel. The VSC-17 system consists of a ventilated concrete cask (VCC) enclosing a multi-assembly sealed basket (MSB) containing spent nuclear fuel as shown in Figure 1. Decay heat generated by the spent fuel is transmitted through the containment wall of the MSB to a cooling air flow. Natural circulation drives the cooling air flow through an annular path between the MSB wall and the VCC liner wall and carries the

heat to the environment without undue heating of the concrete cask. The annular air flow cools the outside of the MSB and the inside of the VCC.

The performance testing consisted of loading the MSB with 17 fuel cans containing consolidated Pressurized Water Reactor (PWR) spent fuel from Virginia Power’s Surry reactors and Florida Power & Light’s Turkey Point reactors. At the time of the cask tests, this fuel was generating about 14.9 kW decay heat. Temperatures of the cask surface, concrete, air channel surfaces, and the fuel compartments (containing the fuel cans) were measured. Testing was performed with vacuum, nitrogen, and helium backfill environments in a vertical cask orientation, with air circulation vents open, partially blocked, and completely blocked. Of these tests, Run #1 (no blocked vents) with helium gas in the MSB was chosen for validation. Detailed descriptions of the VSC-17 experiments, including system geometry, instrumentation locations, specifics of fuel loading, and estimates of the heat generation rates in the spent fuel assemblies are included in the original documentation of the testing [McKinnon, 1992].

Decay Heat Generation for Consolidated Fuel

Individual consolidated fuel cans in the VSC-17 had heat generation rates ranging from 0.707 kW to 1.05 kW. The fuel cans were loaded in the basket to give as close to a symmetrical heat load as possible, with fuel cans near 1.0 kW in the central 3x3 grid, and fuel cans with heat loads near 0.7 kW on the periphery of the basket as shown in [McKinnon, 1992]. Most of the temperature measurements obtained within the fuel cans and the basket are from thermocouples located in one quadrant of the basket. In this quadrant, the peripheral fuel cans all have decay heat values of approximately 0.744 kW, and the inner fuel cans have decay heat values ranging from 0.962 kW to 1.048 kW. The specific heat generation rates for these fuel cans were applied to the homogeneous regions modeling the corresponding fuel cans in a quarter symmetry representation of the MSB.

The decay heat for a given fuel can was applied as a uniform volumetric heat generation rate throughout the homogeneous region, modified only to include an axial power profile based on the measured axial power distribution in the fuel cans as shown in Figure 2. The heat generation is applied over 388 cm (153 inches). The actual heated length for this fuel is estimated at 145.5 inches (i.e., an original length of

144 inches, plus 1.5 inches of growth due to burn-up.) This approximation will result in slightly lower peak fuel temperature predictions than would be obtained if the shorter (actual) heated length were to be used.

The consolidated fuel cans were modeled as non-porous solid using the effective thermal conductivities obtained from the 2-D fluent thermal model of a single assembly.

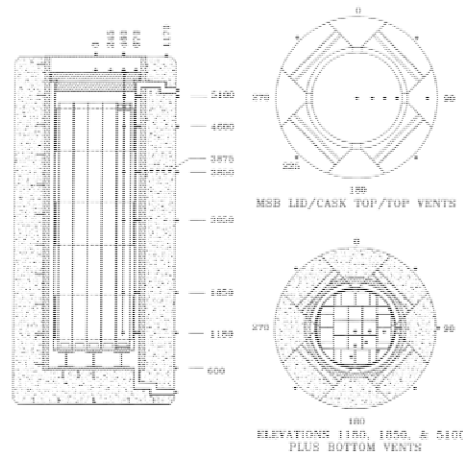


Figure 1 Measurement locations for VSC-17

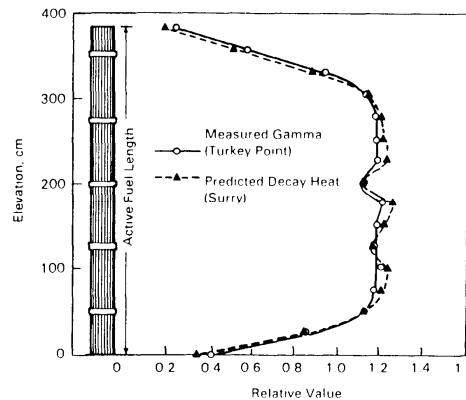


Figure 2 Measured axial decay heat profile

Cases Considered

At first, extended control volume (CV) was used. The control volume included the cask geometry as well as a portion of the surrounding ambient. Two cases using different number of cells were used to check for grid independent solution. The first grid consisted of 1.2 million cells while the second mesh had 2 million cells. In the finer mesh case, the additional cells were placed near the surrounding VCC and MSB walls, the air flow duct and walls

surrounding inert gas flow regions inside the canister. Only the transitional SST $k-\omega$ model was used in this part of the analysis to model the turbulence in the air flow region. As pressure boundaries are used at the inlet and outlet boundaries, an input for operating density is required. As such, in this part of the analysis, cases were created to investigate the effect of operating density on the final results. Most of the analyses performed in this paper used the control volume that includes the dry cask body only without any additional surrounding ambient (i.e. smaller CV). To do so, initially the results obtained from the smaller CV and the extended CV were compared. This step was very important to the rest of the investigations, as the correct operating density for the smaller CV was found. Also, in this part, the measured inlet temperature was checked for consistency. It was noticed through the experimental data, that the average temperature at the inlet was at least 13 degrees higher than the surrounding ambient temperature. This step was of utmost importance, due to the major difference that can be obtained in the final results when different inlet temperature boundary conditions were used. Different cases were run to investigate the influence of different temperatures at the inlet for the smaller CV. The effect of using different turbulence models was investigated using the smaller CV. Among the turbulence models available in Fluent, transitional $k-\omega$ SST, low Reynolds $k-\epsilon$, and standard $k-\epsilon$ models were used to model the flow of air. Laminar model was also used due the low Grashof and modified Grashof in the duct as explained in [Sparrow EM et al., 1985].

Results and Discussions

Three turbulence models as well as a laminar regime were used to model the air flow passage between the MSB and the concrete liner. The first two models among the three chosen turbulence models were the transitional SST $k-\omega$ model and the low-Reynolds $k-\epsilon$ model. Both of these models use damping functions that take into account the effect of the cell Reynolds number on the calculation of the time and length scale of turbulence. Both of these models are used with a fine grid near the wall ($y^+ \sim 1$) to enable integration through the viscosity-affected near wall region. The third chosen turbulence model was the standard $k-\epsilon$ in conjunction with standard wall function to bridge the fully turbulent core region to the viscosity-dominated region near the wall. This model does not use a fine mesh near the wall. In the present application a y^+ close to 20 was used.

Temperature profiles resulting from CFD using the four approaches described above are compared to the experimental data. Axial temperature profile experimental data for different Lances inside the fuel region, liner wall and MSB wall were chosen to compare to calculated CFD results. Additionally, radial profiles from the center of the fuel region to the periphery of the overpack concrete shield at two elevations (3.05 m and 3.85 m) were used to compare the experimental data to the CFD results. Initially, the extended control volume case was used. The studied volume included the cask geometry and a portion of the surrounding ambient. Two types of grids were used to check for grid independent solution. Only the transitional SST $k-\omega$ model was used in this part of the analysis to model the turbulence in the air flow region. Figures 3a through 3c show the CFD temperature distributions along with experimental data. Both grids resulted in the same temperature distribution and, as such, only results from one grid are shown in Figures 3a through 3c.

The extended control volume case was also used to find the appropriate operating density for the smaller CV model (i.e. dry cask only). Fluent user manual [Fluent, 2006] indicates that the operating density should be equivalent to the volumetric average density of the fluid. In the extended control volume, the air volume consists of the extended ambient air and the air sandwiched between the liner and the MSB walls. As the volume of the hot air between liner and MSB walls is negligible compared the represented ambient volume, the average density is closer to the ambient density, and so is the operating density. When the chosen control volume consisted of only the dry cask, the air volume consisted of only the air between the VCC liner and the MSB walls. This air volume continuously removed heat from the MSB wall. As a result the temperature increases from the inlet to the outlet of the cask. The average fluid temperature of this modeled volume is higher than the ambient temperature, and as such, the operating density is lower. The VSC-17 without the ambient (i.e. smaller CV) used the first grid generated for the extended CV but without the cells to model the ambient. The average measured ambient temperature was used at the inlet duct of the smaller CV. The results for this simulation are shown in Figures 4a through 4c. The results were identical to the results obtained for the extended control volume shown in Figure 3a through 3c,

indicating that the problem was correctly modeled (i.e. correct operating density was chosen). The operating density used for this case corresponded to the inlet temperature and not the volumetric average as suggested by Fluent user guide manual [Fluent, 2006]. When the same case was run with the operating density as the average fluid density, the air mass flow entering VSC-17 was 50 % less and the exit air temperature was 12 degrees higher as shown in Table 1. Table 1 also indicates that less heat was absorbed from the fuel rods and the PCT temperature is higher.

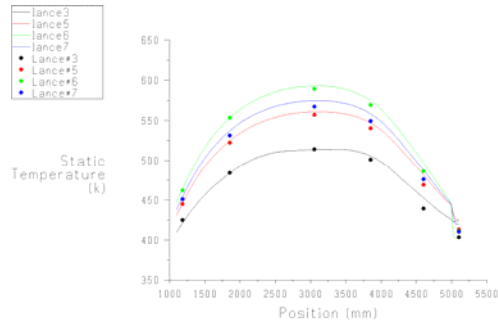


Figure 3a Fuel axial temperature for extended CV using $k-\omega$ SST model. (— CFD, ● Exp).

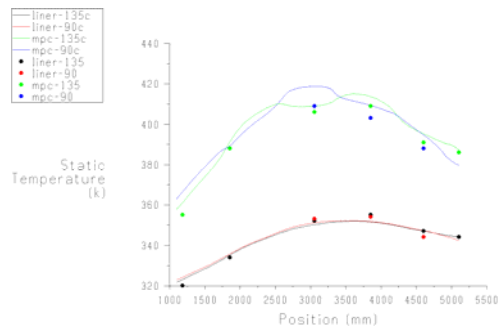


Figure 3b Liner and MSB walls axial temperature for extended CV using $k-\omega$ SST model. (— CFD, ● Exp).

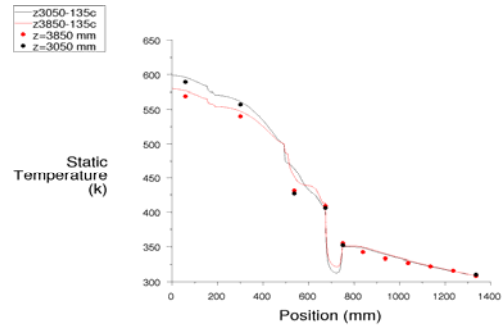


Figure 3c Radial temperatures at two axial locations using extended CV using $k-\omega$ SST model. (—CFD, ● Exp)

If a value for the operating density is not specified, Fluent will use the average density of all the modeled fluids. As in this case, it will use the volumetric average density of both air and helium. As helium density is much lower than air density for the given conditions, the volumetric average density will be even lower than the air volumetric average density. As such, lower air mass flow rate will be induced, and higher PCT will be obtained. The reported

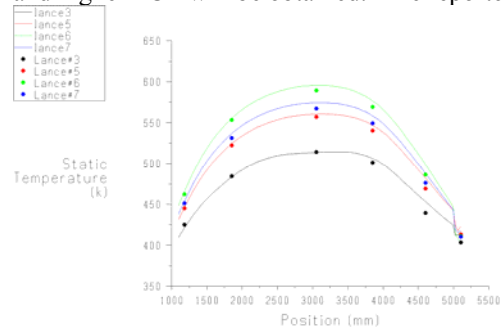


Figure 4a Fuel axial temperature using $k-\omega$ SST turbulence model. (— CFD, ● Exp).

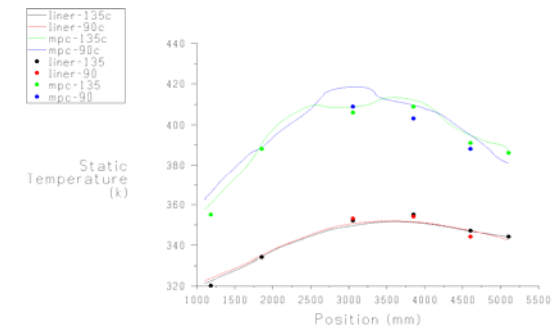


Figure 4b Liner and MSB walls axial temperature using $k-\omega$ SST turbulence model. (— CFD, ● Exp).

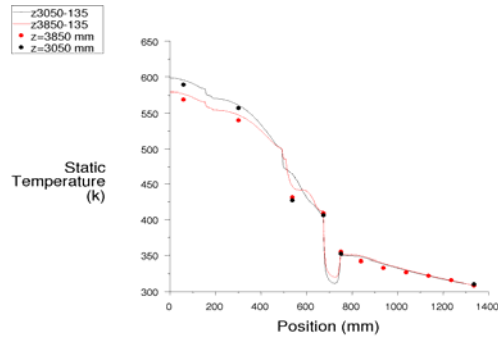


Figure 4c Radial temperatures at two axial locations using $k-\omega$ SST turbulence. (—CFD, ● Exp).

Density (kg/m ³)	PCT (K)	\dot{m}_{air} (kg/s)	Heat absorbed (W)
1 (inlet)	598	0.238	9,284
0.92 (avg)	607	0.1272	7,816

Table 1 Results using varying operating density

measured inlet temperature values were 12 degrees higher than the environment. There are no apparent reasons for the temperature at the inlet to increase. The data indicates an inlet average temperature of 35°C, yet the cask surface temperature just above the inlet is about 27°C. Either the thermocouples at the inlet were reading wrong measurements or they were affected by radiation from the inside of the cask. Either way, these thermocouples were apparently not measuring the correct temperature at the inlet duct of the dry cask. To settle this issue, in the extended CV CFD case, the inlet temperature is not part of the boundary conditions but it is part of the solved domain. Fluent results show that the temperature at the entry of dry cask is identical to the ambient temperature as shown in Table 2.

Control Volume	Turbulence model	T inlet (K)	T exit (K)
Cask + Ambient	Transitional $k-\omega$ SST	296.2	335
Cask	Transitional $k-\omega$ SST	296.2	335
Cask	Low Re $k-\epsilon$	296.2	335
Cask	Std $k-\epsilon$	296.2	333
Cask	Laminar	296.2	335

Table 2 Inlet and outlet air temperature for different turbulence models using ambient inlet temperature.

Table 3 shows the exit temperature for the smaller CV using three different turbulence models. These cases used the average measured inlet temperature as the inlet temperature boundary. The turbulence models used are the low Reynolds $k-\epsilon$ model, the transitional $k-\omega$ SST model and the standard $k-\epsilon$. As shown in Table 3, all the three turbulence models led to the same higher temperature. The resulted exit temperature is 5 degrees higher than the measured average exit temperature. Table 4 shows the exit temperature for the smaller CV using three different turbulence models. These cases used the ambient temperature as an inlet temperature boundary condition. The turbulence models used are the low Reynolds $k-\epsilon$ model, the transitional $k-\omega$ SST model and the standard $k-\epsilon$. As shown in Table 4, all the three turbulence models predicted very well the exit temperature for the smaller CV when compared to the experimentally obtained data. This is yet another proof and indication that the reported measured inlet temperature values do not correctly reflect a realistic inlet temperature. As a result the average measured ambient temperature was used as the inlet temperature for the smaller CV. Figures 4a thru 4c, 5a thru 5c, 6 and 7 show the temperature distributions for different turbulence models. Transitional $k-\omega$

Control Volume	Turbulence model	T inlet (K)	T exit (K)
Cask	Transitional $k-\omega$ SST	308	345
Cask	Low Re $k-\epsilon$	308	345
Cask	Std $k-\epsilon$	308	343

Table 3 Inlet and outlet air temperature for different turbulence models using higher inlet temperature.

CV	Turbulence	\dot{m}_{air} (kg/s)	PCT (K)	Q (W)	T exit (K)
Cask + Ambient	$k-\omega$ SST	0.235	599	9,300	335
Cask	$k-\omega$ SST	0.238	599	9,290	335
Cask	low Re $k-\epsilon$	0.24	597	9,400	335
Cask	Std $k-\epsilon$	0.244	592	9,710	333
Cask	Laminar	0.201	606	8,630	335

Table 4 Results for different turbulence models

SST, low Reynolds $k-\epsilon$, standard $k-\epsilon$, and laminar flow regime were used respectively. The Figures respectively show the axial distribution of the fuel inside the canister, MSB and liner walls. As a first observation, all the four options used to model the

turbulence in the air cooling channel were successful in predicting the location of the peak cladding temperature. The peak cladding temperature value is of great importance in dry cask applications. For long term normal storage conditions, peak cladding temperature is limited to 400°C to avoid fuel cladding deformation caused by excessive creep and to limit the amount of radially oriented hydrides [ISG-11].

Both, the transitional $k-\omega$ SST and the low Reynolds $k-\epsilon$ turbulence models predicted the temperature distribution fairly well in the fuel region inside the canister as well as the passage of cooling air (i.e. MSB and liner walls). Both Figure 4a and 5a show that these two models predicted the location and the value of the peak cladding temperature. Additionally the temperature axial profile of the liner wall and MSB wall were fairly well predicted given the complex nature of this buoyancy driven flow as shown in Figures 4b and 5b. The improvement in the prediction of the liner wall temperature distribution was the result of using a fine mesh near the walls and the capability of these two models to handle low Reynolds turbulent flow. Table 4 shows that when

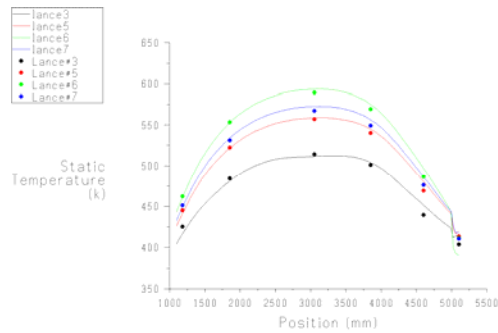


Figure 5a Fuel axial temperature using low Reynolds $k-\epsilon$ turbulence model. (— CFD, ● Exp).

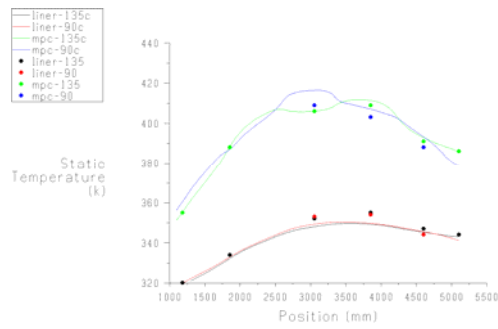


Figure 5b Liner and MSB walls axial temperature using low Reynolds $k-\epsilon$ turbulence model.(— CFD, ● Exp).

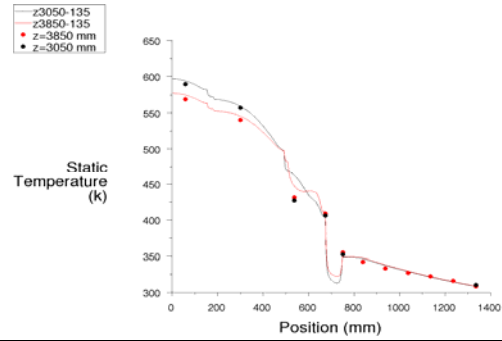


Figure 5c Radial temperatures at two axial locations using transitional $k-\omega$ SST turbulence. (—CFD, ● Exp).

standard $k-\epsilon$ model is used, slightly higher air mass flow rate is induced, thus higher heat rate is absorbed from the cask resulting in a lower air exit temperature. Table 4 shows that when laminar regime is used, a lower air mass flow rate is induced. As a consequence lower heat is absorbed from the cask and higher PCT is predicted. The liner and the MSB wall axial temperature distributions were consistently higher than the experimental data when laminar regime was used as shown in Figure 7. The Standard $k-\epsilon$ model was a better choice than the laminar option, but due to the lack of finer grids near

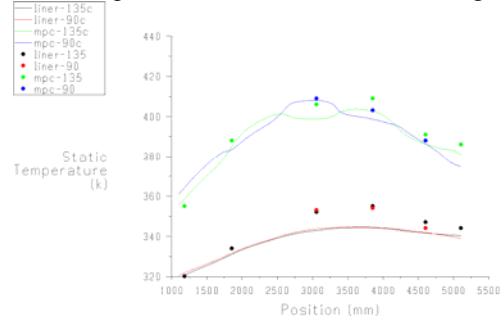


Figure 6 Liner and MSB walls axial temperature using standard $k-\epsilon$ turbulence model. (— CFD, ● Exp).

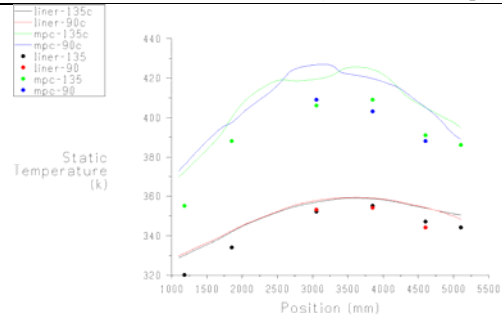


Figure 7 Liner and MSB walls axial temperature using laminar flow regime.(— CFD, ● Exp).

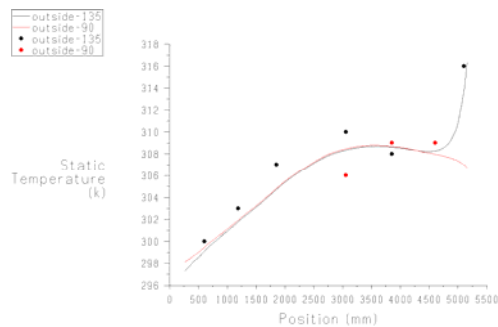


Figure 8 Outside surface temperature using low Re $k-\epsilon$ turbulence model. (— CFD, ● Exp)

the MSB wall and the liner wall, this model was unable to capture the temperature distribution at the liner wall. This model over-predicted the heat exchange between the two walls. Usually, standard $k-\epsilon$ model combined with standard wall function is used when high Reynolds number flow exists. However, this model is not suitable for transitional buoyancy driven flows. The standard $k-\epsilon$ model under-predicted slightly the MSB wall distribution and missed in predicting the liner wall axial distribution. As shown in Table 4 the standard $k-\epsilon$ model over-predicted the heat transfer from MSB wall to the liner, as a result lower temperature will be obtained on the liner wall. The reason behind this is that the standard $k-\epsilon$ is not well suited for low Reynolds number flow and transitional flows. Integration to the wall (i.e. finer grid near the wall) is required to get more information about the wall shear stress and heat transfer for low Reynolds number and transitional flows. In case of transitional Reynolds numbers, as in the case we are dealing with, some type of damping function to enable computation across the laminar viscous sub-layer is required in conjunction with fine mesh near the wall, as was done with the first two turbulence models chosen in this analysis. The standard $k-\epsilon$ under-predicted the liner wall axial temperature distribution as shown in Figure 6, for the reasons enumerated above. Figure 8 shows the outside surface axial temperature distribution using low Reynolds $k-\epsilon$ turbulence model. The CFD analysis followed the trend and predicted correctly the measured temperatures. This Figure shows how well the heat transfer and fluid flow was modeled radially.

CONCLUSIONS

This paper describes the application of the Fluent commercial CFD code to model momentum and energy conservation in a dry cask. As a first step,

temperature measurements for the VSC-17 spent fuel storage cask undertaken by Idaho National Lab (INL) were used to validate the 3-D CFD model. In the validation part, the flow in the air channel is found to be in the transitional region of turbulence. Only turbulence models that are able to deal with this region of the flow regime should be used to perform the analysis. Among the available turbulence models in Fluent, the transitional $k-\omega$ SST and low Reynolds $k-\epsilon$ models were able to predict the experimental data. These models require finer mesh near the wall. The low Reynolds $k-\epsilon$ is preferred because it includes the effect of gravity in the production and dissipation of turbulent kinetic energy. The laminar flow regime overpredicts the PCT and is not appropriate to analyze the air flow. The standard $k-\epsilon$ model is not suitable to model the air flow because it overpredicts the heat transfer from the fuel rods to the air. The flow inside the MSB is laminar. Only laminar flow is appropriate to model flow inside the MSB. When pressure boundaries are used at the inlet and outlet ducts of the dry cask, the operating density should be evaluated at the inlet conditions of temperature and pressure.

REFERENCES:

- 1 McKinnon MA, RE Dodge, RC Schmitt, LE Eslinger, and G Dineen, 1992, "Performance Testing and Analyses of the VSC-17 Ventilated Concrete Cask". TR-100305, Electric Power Research Institute, Palo Alto, California.
- 2 Fluent User Guide Version 6, Fluent Inc, New Hampshire, 2006.
- 3 E. M. Sparrow and L. F. A. Azevedo "Vertical-channel natural convection spanning between the fully-developed limit and the single-plate boundary-layer limit", International Journal of Heat and Mass transfer, Vol.28, No.10, pp.1847-1857, 1985.
- 4 E. M. Sparrow, and A. L. Loeffler, JR "Longitudinal laminar flow between cylinders arranged in regular array", A.I.Ch.E. Journal, Volume 5, No.3, pp325-330, 1959.
- 5 "Cladding Considerations for the Transportation and Storage of Spent Fuel," Interim Staff Guidance -11 (ISG-11), Revision 3, USNRC, Washington D.C.